# Controlled Synthesis and Novel Solution Rheology of Hyperbranched Poly(urea−urethane)-Functionalized Multiwalled Carbon Nanotubes

**Yingkui Yang,[†] Xiaolin Xie,*[,†,‡] Zhifang Yang,[†] Xiaotao Wang,[†] Wei Cui,[†] Jingying Yang,[†] and Yiu-Wing Mai[§]**

*Hubei Key Laboratory of Materials Chemistry and Service Failure, Department of Chemistry, Huazhong University of Science and Technology, Wuhan 430074, People's Republic of China; State Key Laboratory of Polymer Materials Engineering, Sichuan University, Chengdu 610065, People's Republic of China; and Center for Advanced Materials Technology, School of Aerospace, Mechanical and Mechatronic Engineering, J07, University of Sydney, Sydney NSW 2006, Australia*

*Received March 22, 2007; Revised Manuscript Received May 29, 2007*

ABSTRACT: Hyperbranched poly(urea−urethane)s (HPU) were covalently grafted onto the surfaces of multiwalled carbon nanotubes (MWNT) terminated with multihydroxyl groups by a grafting-from technique using one-pot polycondensation of diethanolamine (DEOA) and tolylene 2,4-diisocyanate (TDI). Core−shell nanostructures with MWNT as the hard core and HPU trees as the soft shell were formed after the latter was attached to the former. The grafted-HPU thickness on MWNT could be well-controlled by adjusting the feed ratio of TDI to DEOA. The solution rheology of the HPU-functionalized MWNTs was investigated for the first time by steady shear measurements. Large numbers of proton-donor and proton-acceptor groups were located in the HPU-functionalized MWNT; intra- and intermolecular H-bonds were easily formed by their interactions. At low temperature, shearing forces induce the conversion from intra- to intermolecular H-bonds. Therefore, these solutions exhibited typical shear-thickening behaviors at low shear rates and behaved as Newtonian fluids at high shear rates. At high temperature, H-bonds in the HPU-functionalized MWNT were destroyed, and the packed structures of HPU trees became more loosed. Thereby, the entanglements between two HPU chains, HPU chains and MWNT, and two neighboring MWNTs were formed, which results in an increase in the connectivity and intensity of associated networks with an enhancement in the initial viscosity. With increasing shear rates, disentanglements and orientation of polymer chains and MWNTs lead to shear-thinning at low shear rates and Newtonian behavior at high shear rates. The rheological behaviors of the HPU-functionalized MWNT solutions showed a strong dependence on concentration, temperature, and thermal and shearing prehistory. A mechanism based on H-bond-driven interactions was proposed to account for the novel rheological behaviors of the HPU-functionalized MWNT solutions.

## Introduction

The unique structure-dependent properties of carbon nanotubes (CNTs) have generated an increasing interest ever since their discovery due to their potential applications in molecular devices, (bio)sensors, catalyst supports, electrodes, components in high-performance composites, and many others.[1] However, many applications require functionalization of CNTs to improve their solubility, compatibility, and dispersibility, which allow a better manipulation and processing of insoluble CNTs toward the fabrication of innovative nanodevices and nanohybrids. A number of excellent reviews have been published on the functionalization of CNTs,[2] covering (a) covalent attachment of functional moieties through reaction onto CNTs, (b) noncovalent adsorption or wrapping of various functional molecules, and (c) endohedral filling of their inner empty cavity. Especially, research on functionalization of CNTs with polymers by covalent or noncovalent approaches is rapidly expanding, which is due to the fact that the mechanical and multifunctional properties of polymer/CNT composites are superior to those of conventional polymer-based composites.[3] Since covalent functionalization of CNTs makes the resultant nanocomposites more stable, various linear polymers have been anchored onto the CNT surfaces using grafting-to and grafting-from techniques.[4] However, functionalization of CNTs with well-defined polymers is expected to control over the final properties of polymer/CNT composites. As a grafting-from technique, atom transfer radical polymerization (ATRP) has been successfully performed in the process of functionalized CNTs to control the thickness of grafted polymers.[5] In contrast, the grafting-to approach involves polymer synthesis prior to grafting, which allows to control the length of polymer chains and architecture but results in a low graft density caused by the chains' steric hindrance and relatively low reactivity of groups on CNTs.[6] Recently, Adronov et al. used the well-defined polystyrene and poly(butyl acrylate-*b*-styrene) to functionalize CNTs by copper(I)-catalyzed [3 + 2] Huisgen cycloaddition[4a] and radical coupling reaction,[7] respectively. An in-situ ring-opening polymerization was also applied to control the thickness of the grafted polymer layer onto CNTs by adjusting the feed ratio of monomer to CNT-supported macroinitiators.[8] Research on controlled functionalization of CNTs is being actively studied in many research groups.

Grafting of dendritic polymers on solid substrates has attracted much attention for fabricating novel inorganic/organic hybrids, functional devices, and interfacial materials due to their compact shape, high solubility, low viscosity in bulk and solution, and multifunctional groups and no entanglements in contrast to linear polymer chains.[9] A series of planar or spherical surfaces such as gold,[10] silicon,[11] silica,[12] alumina,[13] and linear polymers[14] have been adopted as supports for dendritic polymers. In the past few years, some research groups have focused on func-

[†] Huazhong University of Science and Technology.
[‡] Sichuan University.
[§] University of Sydney.
* Corresponding author: Tel 86-27-8754-0053; Fax 86-27-8754-3632; e-mail xlxie@mail.hust.edu.cn.

10.1021/ma0707077 CCC: $37.00 
Published on Web 07/07/2007

tionalization of CNTs with dendritic polymers. Sun et al.[15] reported the functionalization of CNTs using dendrons via amidation and esterification and their photophysical properties. Polyamideamine (PAMAM) dendrimers could be well-attached to the CNT surfaces,[16] and formed "nanotube stars",[17] and showed excellent photophysical properties.[18] Hyperbranched polymers were successfully grafted onto CNTs by in-situ ring-opening polymerization of 3-ethyl-3-(hydroxymethyl)oxetane[8b] and self-condensing vinyl polymerization (SCVP) of 2-((bromobutyryl)oxy)ethyl acrylate via ATRP.[5d] Recently, Newkome et al. fabricated a CdS quantum dot composite using dendronized CNT with hyperbranched aminopolyester and studied their photooptical properties.[19] The electrode materials using hyperbranched polyester-functionalized CNTs showed good reversible capacities and excellent capacity retention.[20] These results indicate that functionalization of CNTs with dendritic polymers possesses increased solubility and dispersibility,[15−22] which promise good processing and manipulation ability as well as novel functional properties for CNT hybrids. While large numbers of important works have demonstrated how to functionalize CNTs with linear-structured polymers, there are very few reports on functionalization of CNTs with dendritic polymers.

In addition, polymer grafted CNTs with a core−shell hard−soft nanostructure is expected to give novel solution behaviors because of the structural comparability as compared with those of hairy−rod or rod−coil copolymers.[23] Sano et al. reported that poly(ethylene oxide) (PEO)-functionalized CNTs self-assembled in solutions and in Langmuir−Blodgett (LB) films.[24] Chen et al. found that DNA-functionalized CNTs could form highly branched structures.[25] Recently, Xie et al. showed that PS-grafted CNTs formed nanopins by self-assembly of their solutions whose lengths and diameters increase with concentration.[26] Gao also found that PMMA-grafted CNTs might assemble into basket works, cellular networks, and needles or fibers depending on the solution concentration.[27] However, the solution rheology of polymer-grafted CNTs, especially for hyperbranched polymer-functionalized CNTs, has not been reported to our best knowledge, although the rheology of polymer/CNT composites in their melts[28] and suspensions[29] has been studied.

Recently, hyperbranched grafting is gaining increasing importance owing to their unique properties, relative ease of preparation, and greater availability compared to dendrimers.[9] We synthesized hyperbranched poly(urea−urethane) (HPU)-functionalized multiwalled carbon nanotubes (MWNTs) by polycondensation of tolylene 2,4-diisocyanate (TDI) and diethanolamine (DEOA) in the presence of MWNTs terminated with multiple hydroxy groups.[30] In the present work, we controlled the thickness of the grafted-HPU layers on MWNT by adjusting the feed ratio of TDI to DEOA and investigated the solution rheology of the HPU-functionalized MWNT for the first time by steady shear measurements. For comparison, the solution rheology of linear polystyrene-grafted MWNT (PS-*g*-MWNT) with comparable grafted polymer content was also discussed.

## Experimental Section

**Materials.** Pristine MWNTs (purity >95%, with an average diameter of 50 nm) were purchased from Shenzhen Nanotech Port Co., Ltd. (Shenzhen, China). Tolylene 2,4-diisocyanate (TDI), *N*,*N*-dimethylformamide (DMF), and diethanolamine (DEOA) were distilled by reduced pressure before use. All other chemicals were purchased from Shanghai Reagents Co. and used as received without further purification.

**Measurements.** UV−vis absorption measurements were taken using a Shimadzu UV-2550 diode array spectrophotometer. Fluorescence spectra were recorded on a FP-6500 fluorescence spectrometer. Raman spectra were recorded on a Renishaw laser confocal Raman spectrometer (RM-1000) using a 514.5 nm argon ion laser. Nuclear magnetic resonance (NMR) spectroscopy analyses were carried out on a Unity Inova 600 MHz spectrometer (Varian Co.) using DMSO-$d_6$ as solvent. Thermal gravimetric analysis (TGA) was conducted on a PE TGA-7 instrument with a heating rate of 10 °C/min in an argon flow (20 mL/min). Transmission electron microscopy (TEM) analysis was performed on a Tecnai G 220 electron microscope (PEI Co.) at 200 kV.

Steady-shear viscosities data were collected with a strain-controlled ARES rheometer (TA Instruments) and the measuring shear rates varied from 0.05 to 200 $s^{-1}$. The rheological measurements were carried out at 20, 50, and 80 °C, and all the solutions were preheated for 10 min prior to measurements. The variable-temperature Fourier transform infrared (FTIR) spectra were recorded at 20−95 °C in 15 °C intervals using a Bruker VERTEX 70 spectrometer (KBr disk), and the sample was preheated for 10 min prior to measurements.

**Synthesis of HPU-Functionalized MWNT.** The synthesis of hyperbranched poly(urea−urethane)-functionalized multiwalled carbon nanotubes was described in our recent communication.[30] The synthetic route is shown in Figure 1. The grafting HPU content was controlled by adjusting the feed ratio of tolylene 2,4-diisocyanate (TDI) to diethanolamine (DEOA). Table 1 lists the reaction conditions and selected results as well as the abbreviations used in this paper. Typically, for NTHPU-4, MWNT-OH (0.072 g, 0.20 mmol of −OH groups) was dispersed in DMF (10 mL), and then TDI (3.481 g, 0.02 mol) dissolved in DMF (40 mL) was added dropwise in a nitrogen atmosphere. The reaction mixture was stirred at 0 °C for 12 h. The solution of DEOA (2.102 g, 0.02 mol) in DMF (25 mL) was added dropwise to the mixture of MWNT-OH and TDI with vigorous stirring, followed by keeping at 0 °C for 12 h and at 50 °C for 48 h and then poured into water. The darkish NTHPU-4 powders (0.302 g) were obtained by sequential filtering and washing with DMF until no turbid mass occurred when the filtrate was added dropwise into water. The free hyperbranched poly(urea−urethane)s collected from the filtrate were obtained by precipitation with ice water. IR (KBr, $cm^{-1}$): 3330 (O−H and N−H), 2950−2880 (C−H), 1710 (NH*C*═*O*O, urethane), 1650 (NH*C*═*O*N, urea), 1603 (Ar), 1530 (NH), 1227 (C−N), 1040 (C−O) and 758 (Ar−H). $^1$H NMR (600 MHz, DMSO-$d_6$, ppm): 9.61−8.83 (OCO−N*H*, urethane), 8.60−7.95 (N*H*−CON, urea), 7.71−6.97 (Ar−*H*), 5.47−5.09 (CH$_2$−O*H*), 4.38−4.20 (C*H*$_2$−OCO), 3.62−3.40 (C*H*$_2$−OH), 2.94−2.78 (N−C*H*$_2$), 2.18−1.96 (−C*H*$_3$). $^{13}$C NMR (600 MHz, DMSO-$d_6$, ppm): 156.47−152.43 (all *C*═O in urea and urethane groups), 138.73−112.39 (Ar), 63.81, 62.58 (*C*H$_2$−OCO), 61.92, 60.14 (*C*H$_2$−OH), 51.57, 50.42 (N−*C*H$_2$, linear and terminal units), 47.81, 46.59 (N−*C*H$_2$, dendritic units), and 18.57, 17.42 (−*C*H$_3$). Raman shift (514.5 nm excitation) ($cm^{-1}$): 1356.9, 1586.2, and 1621.9.

**Synthesis of PS-*g*-MWNT.** Polystyrene-grafted MWNT (PS-*g*-MWNT) was synthesized by the in-situ free-radical polymerization of styrene in the presence of MWNT terminated with vinyl groups as described in our other paper.[26] TGA measurements showed the grafted polystyrene content in PS-*g*-MWNT was 86.3 wt %.

## Results and Discussion

**Controlled Synthesis and Characterization.** It is generally accepted that the molecular weight of the resulting polymer can be controlled by adjusting the molar feed ratio of the monomers in a polycondensation process. We conducted four experiments with different feed ratios of TDI to DEOA to synthesize the HPU-functionalized MWNT (Table 1). Figure 1 represented the synthesis procedures. The bis-hydroxyl-functionalized MWNT (MWNT-OH) was induced onto the MWNT surfaces by reacting the acid-oxidized MWNT (MWNT-COOH) with excess thionyl

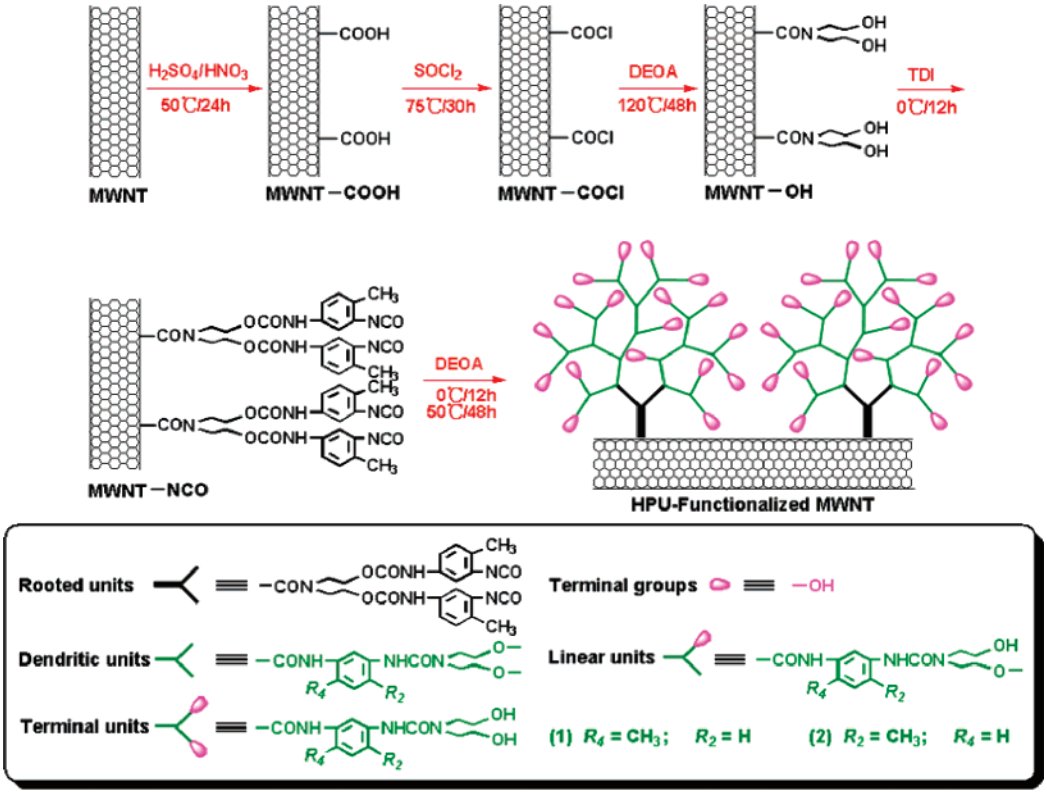


**Figure 1.** Synthesis of the HPU-functionalized MWNT and chemical structures.

**Table 1. Functionalization of MWNT with HPU and Selected Results**

| sample | $R_{wt}$[a] | $R_{mol}$[b] | yield/ wt %[c] | polymer/ wt %[d] | $d$/nm[e] | DB[f] |
|---|---|---|---|---|---|---|
| NTHPU-1 | 48:1 | 1.15:1.00 | 9.6 | 40.6 | 4.2 | 0.53 |
| NTHPU-2 | 48:1 | 1.10:1.00 | 13.5 | 60.5 | 7.1 | 0.56 |
| NTHPU-3 | 48:1 | 1.05:1.00 | | 72.7 | 11.2 | |
| NTHPU-4 | 48:1 | 1.00:1.00 | 10.3 | 83.5 | 14.5 | 0.63 |

[a] $R_{wt}$ = TDI:MWNT-OH (wt:wt). [b] $R_{mol}$ = DEOA:TDI (mol:mol). [c] The yield calculated by the equation $(W_a/W_b) \times 100\%$, where $W_a$ is the weight of the HPU-functionalized MWNT and $W_b$ is the weight of free HPU collected from the reaction solution. [d] The grafted-HPU content calculated by TGA. [e] The average thickness of the grafted-HPU layer measured by TEM. [f] The DB of free HPU calculated by NMR data.[30]

chloride and then excess DEOA. The high-density hydroxyl groups (ca. 2.8 mmol $g^{-1}$ of MWNT-OH) can increase the reactivity of MWNT to better anchor the HPU trees onto MWNT. When TDI is added dropwise to the suspension of MWNT-OH, the 4-NCO in TDI reacts preferentially with the OH group of MWNT-OH to afford the NCO-group-functionalized MWNT (MWNT-NCO). The inherent reactivity of the NH group is higher than that of the OH group in DEOA, and that of 4-NCO than 2-NCO in TDI,[31] which provides an essential feature enabling selective sequential reactions to yield the HPU-functionalized MWNT. It should be noted that the coupling reaction between the two MWNT-OHs through TDI is impossible due to the excess TDI relative to MWNT-OH and the difficult motion of MWNT-OH. Similarly, there is no possibility that two MWNT-NCOs are connected by DEOA because the collision reaction between MWNT-NCO is relatively difficult owing to the low concentration (1.8 mg/mL) and low temperature (0 °C) as well as the difficult motion of the rigid MWNTs. Also, the molar mass of functional groups (NH and OH) in DEOA exceeds that of TDI. Moreover, the fraction of the HPU-functionalized MWNT relative to the free HPU collected from the reaction solution is small (Table 1) due to the large feed ratio of monomer to MWNT-OH. In contrast, the collision reaction between oligomers is easier than that of oligomer and MWNT-NCO owing to the steric effect of the latter. In fact, the yield of the polymer-functionalized CNTs relative to the free polymers is generally very low in the current study.[8]

FTIR, NMR, and Raman spectroscopy revealed that hyperbranched poly(urea−urethane)s were covalently attached to MWNT (Supporting Information). A control experiment of blending MWNT-OH with neat HPU was also conducted to further confirm the covalent linkage between the HPU trees and MWNT, in which the entangled MWNT and free polymers formed two different phases and no coated polymer layers were observed on the MWNT surfaces from TEM images. The resultant HPU-functionalized MWNT shows good solubility in DMF, DMAC, NMP, and DMSO due to the HPU trees grown from MWNT.[30]

The content of the grafted-HPU in the HPU-functionalized MWNT can be easily detected by TGA measurement, as shown in Figure 2. TGA trace of crude MWNT shows little weight loss, and neat HPU gives full weight loss at 600 °C. Therefore, the relative amounts of grafted-HPU can be determined. The grafted-HPU content increases from 40.6 to 83.5 wt % as the feed ratio of TDI to DEOA ($R_{mol}$) falls from 1.15:1.00 to 1.00:1.00 (Table 1). A detailed insight into the changes in the grafted density can be further deduced from ultraviolet visible (UV−vis) and fluorescence spectroscopy. Figure 3 represents the UV−vis spectra of NTHPU-1, NTHPU-2, NTHPU-3, and NTHPU-4 and neat HPU solutions in DMF with the same concentration of 0.25 mg/mL. The UV−vis spectra show featureless absorption starting from 300 nm decreasing monotonically up to 800 nm, which is characteristic of the solubilized MWNT, in agreement with its deeper color.[32] The absorption intensities at 400 and 500 nm vs the loaded MWNT content indicate that the absorption intensity is inversely proportional to the content of grafted-HPU present in the HPU-functionalized MWNT. Figure 4 shows the fluorescence spectra of NTHPU-1, NTHPU-2,

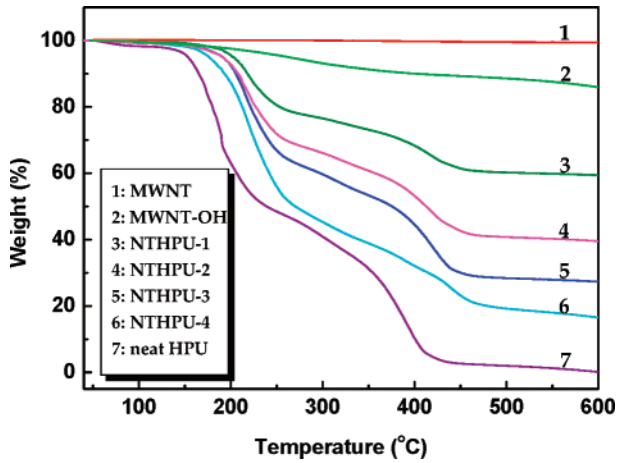


**Figure 2.** TGA curves of pristine MWNT, MWNT-OH, the HPU-functionalized MWNT, and neat HPU.

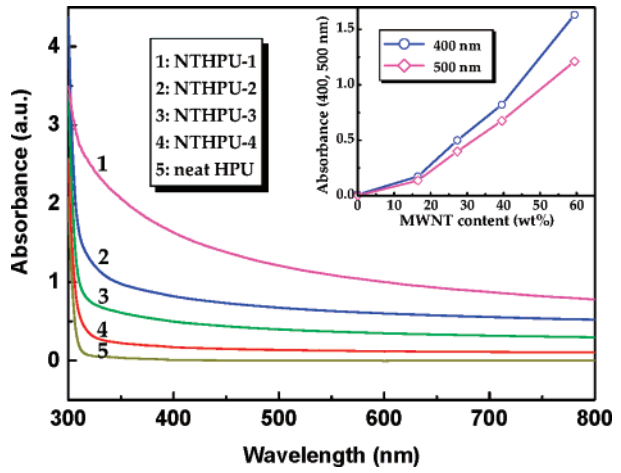


**Figure 3.** UV−vis spectra of NTHPU-1 (1), NTHPU-2 (2), NTHPU-3 (3), NTHPU-4 (4), and neat HPU solutions (5) in DMF with the same concentration of 0.25 mg/mL. The inset shows that the absorption value at 400 and 500 nm was plotted against the loaded MWNT content.

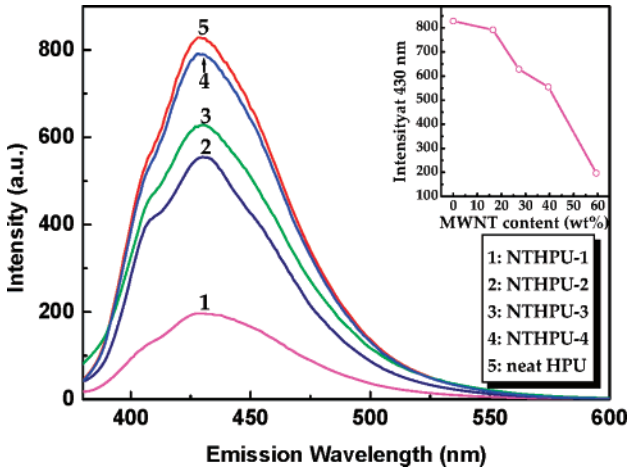


**Figure 4.** Fluorescence emission spectra of NTHPU-1 (1), NTHPU-2 (2), NTHPU-3 (3), NTHPU-4 (4), and neat HPU (5) solutions in DMF with the same concentration of 0.1 mg/mL (excited at 360 nm). The inset shows that the fluorescence intensity at 430 nm was plotted against the loaded MWNT content in the HPU-functionalized MWNT.

NTHPU-3, and NTHPU-4 and neat HPU solutions in DMF with the same concentration of 0.1 mg/mL. Upon excitation at 360 nm, the emission of the HPU-functionalized MWNT is significantly quenched relative to neat HPU solution with a maximum emission peak of 430 nm, indicating an intermolecular interaction between the grafted-HPU and MWNT.[33] The decrease in fluorescence intensity confirms that there is photoinduced electron transfer from the grafted-HPU to MWNT, in which the grafted-HPU trees act as energy-absorbing and electron-transferring antennae and the nanotubes act as electron acceptors.[34] As seen in the inset of Figure 4, the fluorescence intensity at 430 nm decreases with increasing MWNT content, indicating that the higher amount of grafted polymer in the HPU-functionalized MWNT has much higher quantum yield.[35]

The most direct evidence for controlled functionalization of MWNT with HPU is obtained by TEM images, as given in Figure 5. The acid oxidized MWNT (MWNT-COOH) retains its tubular structure with almost smooth surfaces and cap opening (Figure 5A). For the HPU-functionalized MWNT, core−shell nanostructures with HPU layers as shell and MWNT as core are clearly observed. The average thickness of the HPU layers on the MWNT surfaces is ∼3.7, ∼7.1, ∼11.2, and ∼14.5 nm for NTHPU-1 (Figure 5B), NTHPU-2 (Figure 5C), NTHPU-3 (Figure 5D), and NTHPU-4 (Figure 5E), respectively. Compared to the dense MWNT-COOH, a relatively loose network of nanotubes can be seen in the HPU-functionalized MWNT caused by physical entanglement or hydrogen-bonding between different MWNTs due to their large length-to-diameter ratios. Moreover, some protuberances are also seen on the MWNT surfaces in the high magnification TEM image (Figure 5F) because of the globular-shaped structure of hyperbranched polymers. Therefore, TEM observations are consistent with the aforementioned results of TGA, UV−vis, and fluorescence spectra, confirming the thickness of the grafted-HPU layers on MWNT can be efficiently controlled by adjusting the feed ratio of TDI to DEOA.

The degree of branching (DB) of free HPU collected from the reaction solution was further determined by NMR spectroscopy[30,36] and summarized in Table 1. But these values are considerably higher than the maximum value (DB = 0.5) predicted by theory.[37] Frey et al.[38] pointed out that the equation proposed by Fréchet et al.[36] leads to an overestimation of the DB. However, this difference might be related to the slow monomer addition in our experiment. Frey[39] and Müller[40] et al. already showed that the DB can be enhanced from 0.5 to 0.66 via the slow monomer addition procedure. Also, according to the polycondensation mechanism and some publications,[8,30] we believe the molecular structure of HPU grafted to MWNT is similar to that of free HPU in the solution. It can be seen that the DB increases with increasing grafted-HPU content in the HPU-functionalized MWNT. However, the greater content of grafted-HPU is consistent with the higher molecular weight of HPU due to their same reactivity sites on MWNT toward the grown HPU trees. This implies that the DB increases with increasing molecular weight, which is in very good agreement with theoretical predictions[38,41] and experimental results.[8,42]

**Hydrogen Bonds.** Since there are large numbers of proton-donor groups (i.e., O−H and N−H) and proton-acceptor groups (i.e., C═O, C−N, and O−H) in the dendritic, linear, and terminal units in the HPU-functionalized MWNT, intra- and intermolecular H-bonds are easily formed by interactions between proton-donor and proton-acceptor groups, such as C−O···H−O, C═O···H−N, and H−O···H−O. Figure 6 shows the variable-temperature FTIR of NTHPU-4, which shows two bands in the 3600−3000 $cm^{-1}$ region (Figure 6a), whereby the weak and narrower shoulder band at 3412 $cm^{-1}$ corresponds to free O−H and N−H groups, and the broad peak at ca. 3300 $cm^{-1}$ is attributed to the wide distribution of the hydrogen-

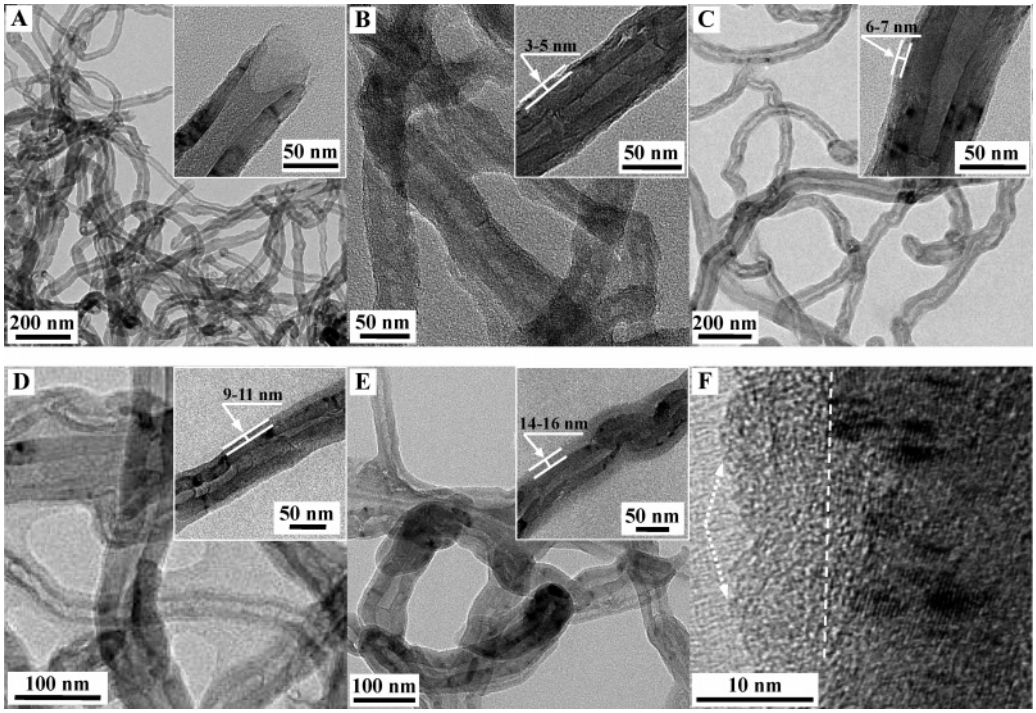


**Figure 5.** TEM images of MWNT−COOH (A), NTHPU-1 (B), NTHPU-2 (C), NTHPU-3 (D), and NTHPU-4 (E, F).

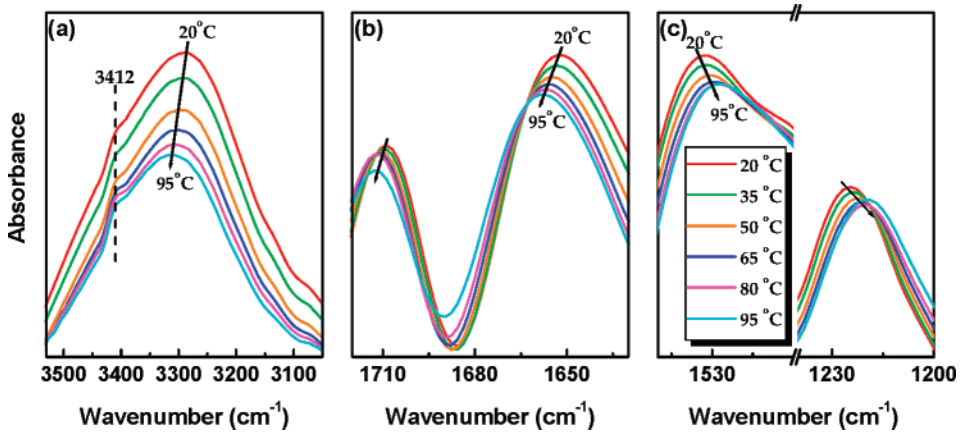


**Figure 6.** Variable-temperature (20−95 °C) FTIR spectra in the (a) O−H and N−H stretching, (b) C═O (amide I) stretching, (c) N−H wagging (amide II), and C−N stretching (amide III) regions of NTHPU-4. Arrows indicate the direction of increasing temperature.

bonded O−H (C−O···H−O and H−O···H−O) and N−H (C═O···H−N) groups. As the temperature increases from 20 to 95 °C in 15 °C intervals, the center of the broad peak for O−H and N−H stretching shifts to higher frequency (i.e., from 3288 $cm^{-1}$ at 20 °C to 3344 $cm^{-1}$ at 95 °C) with weakened absorbance, since higher annealing temperatures tend to disrupt the hydrogen-bonding interactions.[43] Similar changes can be observed in the C═O (amide I) stretching regions (Figure 6b). With increasing temperature from 20 to 95 °C, the C═O stretching within urethane and urea groups shift systemically to higher wavenumber from 1708 to 1712 $cm^{-1}$ and from 1650 to 1658 $cm^{-1}$, respectively, as a result of weakening in H-bonds. On the contrary, the N−H wagging (amide II) and C−N stretching (amide III) shift distinctly to lower frequency (Figure 6c). The wavenumber of N−H band is reduced from 1535 to 1527 $cm^{-1}$ and that of the C−N band from 1225 to 1217 $cm^{-1}$. These are consistent with the result that the wavenumber of hydrogen-bonded C═O bond is smaller than that of free C═O bond, while the wavenumber of hydrogen-bonded N−H wagging is larger than that of free N−H wagging.[44] Hence, the associations and disassociations of H-bonds are controlled by temperature, and the H-bond interactions can be weakened with increasing temperature.

**Solution Rheological Behaviors.** Figure 7 shows the effects of grafted-HPU content, shear rate, and temperature on the viscosity of HPU-functionalized MWNT, PS-*g*-MWNT, and neat HPU solutions in DMF with the same concentration (5.0 mg/mL). At ambient temperature (20 °C) and low shear rates (0−50 $s^{-1}$) (Figure 7a), the solutions of HPU-functionalized MWNT and neat HPU exhibit non-Newtonian shear-thickening behaviors, in which the viscosities increase sharply with increasing shear rates. At high shear rate (50−200 $s^{-1}$), Newtonian behaviors are observed with steady shear viscosities independent of shear rates. At intermediate temperature (50 °C) (Figure 7b), similar phenomena for the NTHPU-3, NTHPU-4, and neat HPU can also be seen. However, NTHPU-1 with the lowest content of grafted-HPU shows shear-thinning at low shear rates and Newtonian behavior at high shear rates at intermediate temperature. At higher temperature (80 °C) (Figure 7c), severe shear-thinning at low shear rates and Newtonian behavior at high shear rates are detected for all samples. In the range of temperature studied, the greater the grafted-HPU content in the

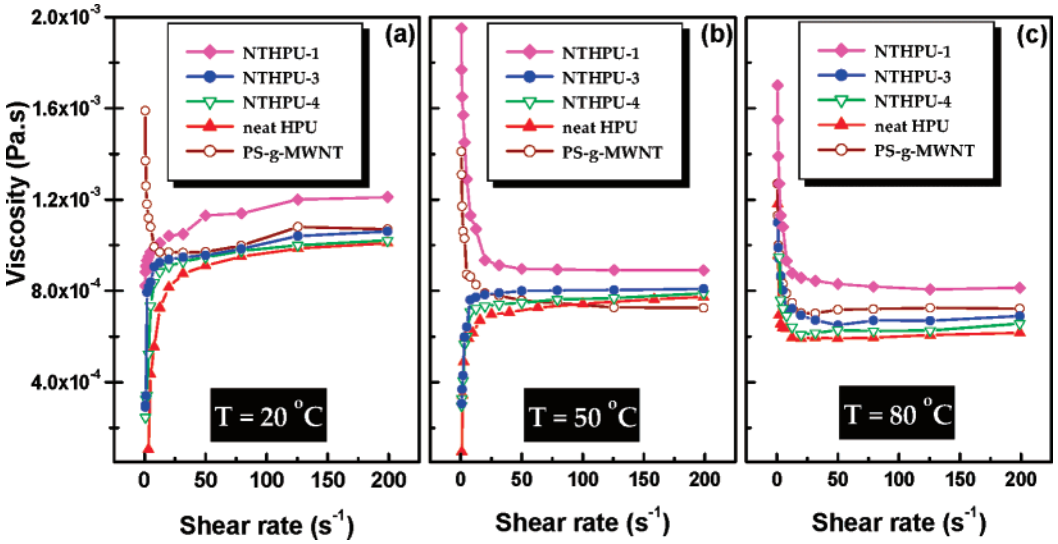


**Figure 7.** Viscosity as a function of shear rate for the HPU-functionalized MWNT, PS-*g*-MWNT, and the neat HPU in DMF for temperature ranging from 20 to 80 °C. The solution concentration is 5.0 mg/mL.

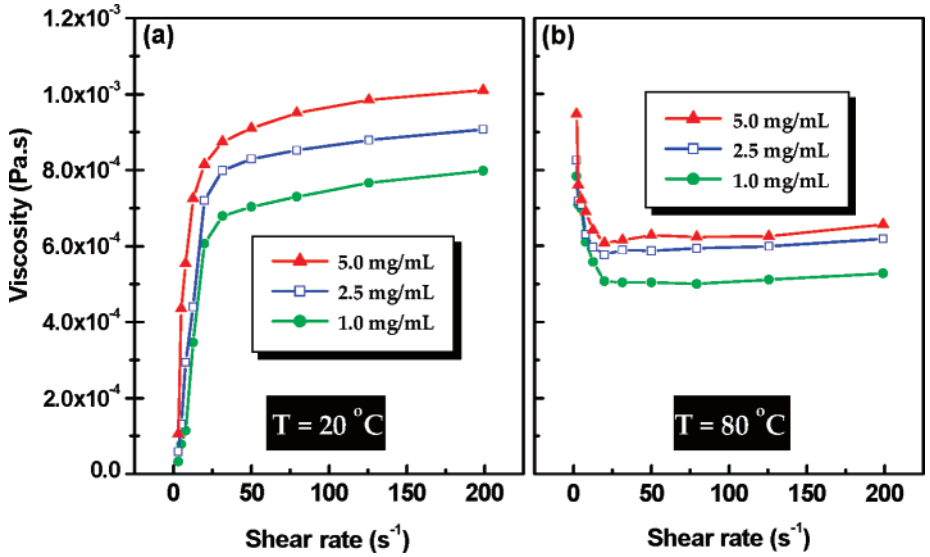


**Figure 8.** Viscosity as a function of shear rate for the NTHPU-4 sample in DMF solution with the different concentrations.

HPU-functionalized MWNT, the lower is the solution viscosity. For comparison, the solution behavior of PS-*g*-MWNT is included in Figure 7. Clearly, PS-*g*-MWNT solution always exhibits shear-thinning at low shear rates and a shear rate-independent viscosity at high shear rates. It is noticed that the solution viscosities of NTHPU-3, NTHPU-4, and HPU in the Newtonian regions (above 100 $s^{-1}$) are lower than those of PS-*g*-MWNT, whereas NTHPU-1 solution shows the highest viscosity. In addition, the solution viscosities for all samples decrease as temperature increases.

Figure 8 shows the effect of solution concentration on the rheology behavior of the HPU-functionalized MWNT at different temperature. For NTHPU-4 solution, the viscosity increases with increasing solution concentration in both regions of shear-thickening (Figure 8a) and shear-thinning (Figure 8b). The NTHPU-4 solution behaviors at a given concentration (2.5 mg/mL) under cycled temperature and shearing were also examined to investigate the effect of thermal and shearing history on the solution rheology (Figure 9). The solution viscosity of NTHPU-4 was measured at 20 °C as a function of increasing shear rate (curve 1). Then, the temperature was raised to 80 °C, kept there for 15 min, and cooled to 20 °C again. The viscosity was recorded again varying with shear rate as shown by curve 2. It can be seen that cycled temperature and shearing have no evident effect on the rheology profile with shear-thickening at low shear rates and Newtonian behavior at high shear rates. However, the viscosity values in curve 2 are much higher than those in curve 1, though they are all measured at the same temperature of 20 °C.

**Rheological Mechanism.** It has been reported that dendrimers exhibit Newtonian behavior in solutions[45] and their melts[46] over a wide range of shear rates due to the lack of chain entanglements. Hyperbranched polyesters also display Newtonian behaviors like dendrimers in solution despite their irregularities in molecular architecture.[47] Computer simulation has shown that the peripheral chains of hyperbranched polymers might participate in entanglements of chains.[48] Fréchet found that Boltorn hyperbranhced polyesters demonatrated shear-thinning or Newtonian behaviors depending on the generation number.[49] Later, McHugh et al. also found that hyperbranched poly(ether−imide)s (HBPEI) promoted a significant degree of coil overlap and entanglement coupling and exhibited Newtonian behavior at low molecular weight and shear-thinning at high molecular weight.[50] However, shear-thickening effects were rarely ob-

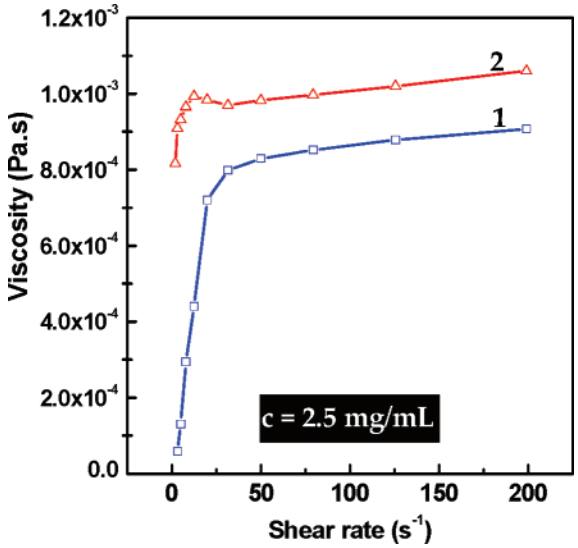


**Figure 9.** Solution rheological behavior of NTHPU-4 under the cycled temperature and shearing prehistory.

served in common polymer solutions or melts, but they are well-known to occur in complex fluids including concentrated suspensions[51] and associated polymers.[52] In general, shear-thickening behaviors are related to shear-induced changes of the fluid microstructure, such as shear-induced cross-linking,[53] shear-induced non-Gaussian chain stretching,[54] and network reorganization.[55] Why does a complex system of hyperbranched polymers functionalized MWNT, containing H-bonds and rigid-rod-like MWNT, show the aforementioned novel rheological behavior? We propose a possible mechanism to account for the rheological phenomena of the HPU-functionalized MWNT solutions, as shown in Figure 10.

At ambient temperatures (20 °C) without any shear flow (Figure 10a), HPU-functionalized MWNTs are randomly distributed in solutions. And the grafted-HPU trees adopt a rather compact conformation due to their own globular structures and intramolecular aggregate, in which mainly two types of intramolecular H-bonds are formed by the interior of a single HPU tree and two neighboring HPU trees on a single nanotube. After applying a low shear rate, the compact conformation of the HPU trees in solutions becomes much loosened compared to their original states due to the partial disassociations of intramolecular H-bonds under shear flow.[56] As the shear rates increase, the disassociations of intramolecular aggregates and partial replacement by intermolecular ones under shear lead to the formation of a transient cross-linked network with large hydrodynamic volumes (Figure 10b). In a shear field, the larger object dissipates more energy, resulting in a higher viscosity.[47] In 1955, Eliassaf et al.[56] already observed a drastic increase in viscosity of poly(methacry1ic acid) (PMA) upon agitating a PMA solution owing to the shear-induced intermolecular cross-linking by hydrogen-bonding between carboxyl groups on neighboring PMA chains. Continuing increase in shear rates results in stretching and extension of the HPU chains, exposing more hydrogen-bonding groups on the MWNT surfaces, which undergo intermolecular H-bonds in the HPU trees on the adjacent MWNT surfaces and thus induce conversion from intra- to intermolecular H-bonds. When the shear rates reach a critical value, the functionalized MWNTs are fully extended and aligned along the flow direction, resulting in an intermolecular H-bond-stabilized network, with a drastically enhanced viscosity (Figure 10c). Further, shearing force induces the deformation of flexible coils to an extent that results in nonlinear retraction forces due to stiffening of the flow-stretched macromolecules and also leads to an increased viscosity.[57] Thereafter, the steady rheological microstructure is maintained, which shows a Newtonian behavior with further increasing shear rates. Similar shear-induced associations have been invoked to explain the shear-thickening properties of hydrophobically modified polymers[58] and polyelectrolyte solutions.[59]

When the HPU-functionalized MWNT solutions are heated to 50 °C from 20 °C, intramolecular H-bonds in NTHPU-3 and NTHPU-4 are partly weakened (Figure 10d), but their solutions still show similar rheological behaviors as at 20 °C. With increasing shear rates, the residual intramolecular associations are transformed into intermolecular associations (Figure 10e). However, their viscosities are systematically lower than those of their solutions at 20 °C. This can be attributed to three factors: (a) Higher temperature induces the disassociations of H-bonds and increases the mobility of the functionalized MWNTs, which result in unfolding of polymer chains and weakening of associated networks due to their thermal sensitivity. (b) Higher temperature increases the solubility of the functionalized MWNTs due to entropy reasons and induces also a decrease in solvent viscosity. (c) Both weakened H-bonds and increased solubility might reduce the friction coefficient between segments of the functionalized MWNTs, which enables better orientation of the functionalized MWNTs under shear flow. The combined effect of these three contributions lowers the magnitude of shear-thickening showing a lower viscosity as a result.

At high temperature (80 °C), the solutions of the HPU-functionalized MWNT and neat HPU show shear-thinning behaviors, differing greatly from previous shear-thickening. This is because the packed structures of HPU trees become more loosened owing to the breakage of intramolecular H-bonds caused by increasing temperature (Figure 10f);[43,60] the entanglements between two polymer chains, polymer chains and MWNT, and two neighboring MWNTs are formed, which leads to an increase in the number of junctions and a great enhancement in initial viscosity as compared with their solutions at lower temperature. With increasing shear rates, these entanglements are unlocked, grafting polymer chains and MWNT are gradually oriented along the shear direction, which leads to a decrease in solution viscosity. After the above disentanglements and orientation are completed under shear (Figure 10g), the solution viscosity tends to a steady value with a Newtonian fluid similar to the rheology of associated polymers.[52a] Moreover, for NTHPU-4 at a given concentration (2.5 mg/mL), as shown in Figure 9, a prominent increase (curve 2) in viscosity as compared with the starting solution (curve 1) is observed after undergoing a thermal and shear cycle. This behavior is related to the irreversible deformation, in which intramolecular H-bonds are completely destroyed at 80 °C, and the neighboring HPU-functionalized MWNTs are nearing each other under shear flow. After the temperature is cooled to 20 °C, higher density intermolecular H-bonds are formed. With increasing shear rates, the connectivity and intensity of H-bond networks (Figure 10c) increase, which will strengthen the interaction with functionalized MWNTs with an increased viscosity.

As shown in Figure 7, at a given concentration, the solution viscosity of the HPU-functionalized MWNT increases as the grafted-HPU content decreases or the MWNT content increases. It is well accepted that hyperbranched polymers have higher solubility and lower viscosities compared with those of linear analogues.[9] In those systems of hyperbranched polymers grafted linear polymers or their blends, their viscosities also decrease with increasing content of hyperbranched polymers.[47] Since a

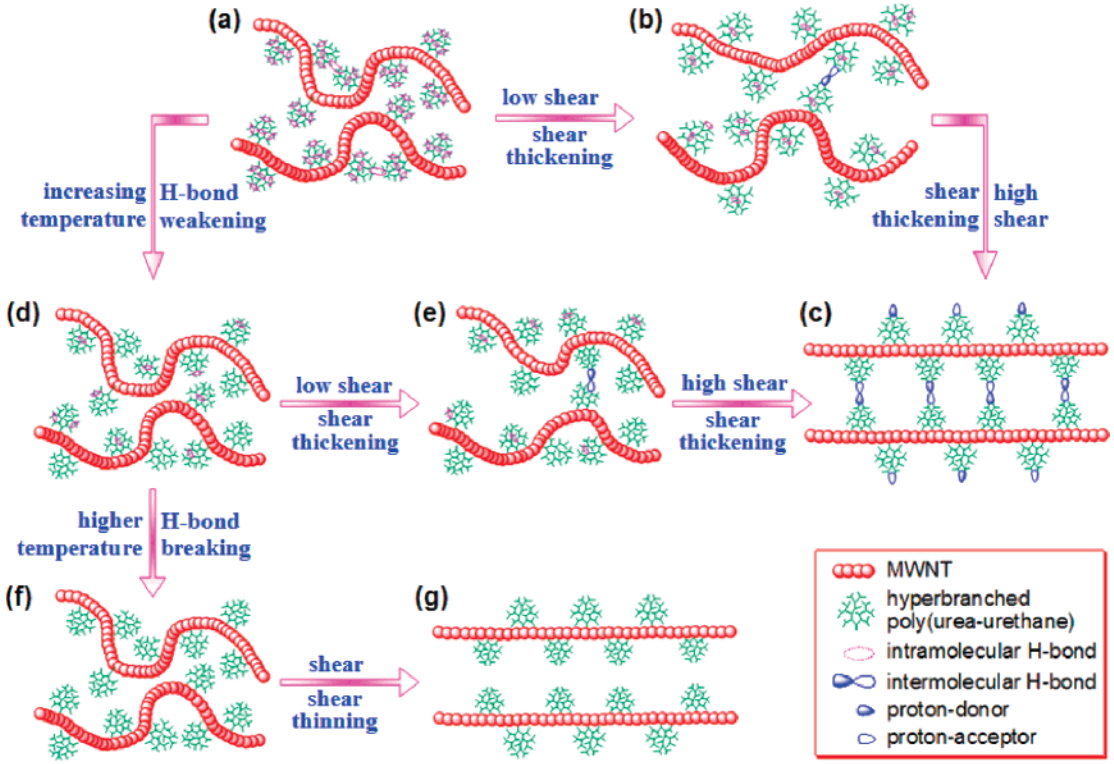


**Figure 10.** Rheological mechanism of the HPU-functionalized MWNTs in their solutions.

single CNT can be regarded as a large-scale linear inorganic−polymer chain,[23a] the HPU-functionalized MWNT is regarded as hyperbranched polymers grafted linear MWNT. In a way, the increasing viscosities are due to the increasing content of linear MWNT within the HPU-functionalized MWNT, but this is not sufficient explanation because of the existence of the additional H-bonds in these systems. In addition, the DB has also been found to affect the rheological properties of hyperbranched polymers.[61] The lower grafted-HPU content has a shorter HPU chain due to their same reactivity sites on MWNT toward the grown HPU trees. Therefore, the higher MWNT content in the HPU-functionalized MWNT involves fewer interactions of H-bonds due to the short HPU chains, resulting in a loss of connectivity in the associated networks, which will induce a lower viscosity. In contrast, however, the decreasing content of grafted-HPU in the HPU-functionalized MWNT will lead to an increased viscosity, similar to those of hyperbranched polymers grafted linear polymers.[47] Moreover, the grafted-HPU with a lower DB in the functionalized MWNT also exhibited a higher viscosity. Hence, the influence of increasing the MWNT content on its solution viscosity is much stronger than that of less H-bond interactions, the solution viscosities are gradually increased as a result. Especially, the most pronounced shear-thinning effect is observed early for the lowest content of the grafted-HPU (NTHPU-1) with the lowest DB at moderate temperature (Figure 7b). Because the number of H-bonds in NTHPU-1 is least, H-bond interactions are easily destroyed by moderate temperature and consecutive shearing. Another reason is its low DB that also tends toward shear-thinning similar to that of linear polymers. Moore et al. reported that onset of shear-thinning appeared at lower shear rates as DB was decreased for hyperbranched aromatic poly(ether imide)s.[61b]

As shown in Figure 8, the NTHPU-4 solution exhibits an evident increase in viscosity with increasing concentration. This phenomenon is frequently observed for associated polymers.[63] As the concentration increases, the number of the functionalized MWNT per unit volume in solution increases. At lower concentration, the functionalized MWNTs have less chance of interaction with each other by H-bonds. Hence, the interaction of intramolecular H-bonds is dominant compared to intermolecular associations, which produces a decrease in the hydrodynamic radius, explaining the lower viscosity. Moreover, the interaction of H-bonds is broken more easily than that of covalent bonds, and the re-formation of broken H-bonds however requires that the polar groups of molecular chains come within the interacting distance (2−5 Å).[64] Therefore, with increasing concentration, the formation of intermolecular H-bonds becomes more probable, which results in the creation of a network structure of functionalized MWNTs with large hydrodynamic volumes, giving a higher viscosity. Thus, the interaction of intramolecular H-bonds dominates at low concentration, whereas that of intermolecular H-bonds dominates at higher concentration. Even when the H-bonds are destroyed, the increasing concentration also makes the polymer chains on the MWNT surfaces and nanotubes themselves overlap and entangle with neighboring ones, resulting in formation of large hydrodynamic volumes with higher viscosity.

Unlike the HPU-functionalized MWNT solutions, no shear-thickening is observed in PS-*g*-MWNT solutions (Figure 7). The different behaviors are due to the differences in the polymer structures. The solution of PS-*g*-MWNT behaves as shear-thinning at low shear rates followed by Newtonian behavior at higher shear rates. Since polystyrene is a linear polymer and nanotube is a linear macromolecule, we can consider PS-*g*-MWNT as a large-scale linear copolymer chain. Thus, shear-thinning mechanism of linear polymers will apply to explain the observed rheological behavior. For the starting solution of PS-*g*-MWNT, the formation of large numbers of entanglement points between PS chains, PS and nanotubes as well as nanotubes themselves results in a high initial viscosity. When shear forces are applied, some entanglements are gradually disrupted. With increasing shear rates, the transient networks

formed by physical entanglements are broken up, and the viscosity drops sharply. At higher shear rates, the alignment and orientation of PS-*g*-MWNT make the viscosity fall even further until shear orientation is fully developed. Therefore, no deformation takes place in the system as a result of a Newtonian fluid. Additionally, the NTHPU-4 solution shows a lower viscosity relative to that of PS-*g*-MWNT with comparable grafted polymer content, which is due to a smaller hydrodynamic volume for hyperbranched polymers as compared with linear polymers, resulting in a lower viscosity.

## Conclusions

MWNT has been functionalized with hyperbranched poly(urea−urethane)s (HPU) by a grafting-from approach using one-pot polycondensation of TDI and DEOA. The thickness of the grafted-HPU on MWNT is controlled by adjusting the feed ratio of TDI to DEOA. At low (20 °C) and moderate (50 °C) temperatures, shearing force induces the conversion from intra- to intermolecular H-bonds in the HPU-functionalized MWNTs; thereby their solutions exhibit typical shear-thickening behaviors at low shear rates and Newtonian behaviors at high shear rates. However, at high temperature (80 °C), H-bonds in the HPU-functionalized MWNTs are destroyed, and the packed structures of HPU trees on MWNTs become loosened and their solutions showed shear-thinning at low shear rates followed by Newtonian fluids at high shear rates. At a given concentration for the HPU-functionalized MWNT, their solution viscosities increase as the grafted-HPU content decreases or the MWNT content increases. Also, their solution viscosities have strong dependence on concentration and temperature and are related to the thermal and shearing prehistories. In contrast, the solutions of PS-*g*-MWNT with comparable polymer content presented typical shear-thinning behaviors at low shear rates and Newtonian fluids at high shear rates over the range of the tested temperatures.

**Acknowledgment.** We are grateful for the financial support of the National Natural Science Foundation of China (20474021), National Basic Research Program of China (61337), Program for New Century Excellent Talents in Universities of China (NCET-05-0640), Open Project of State Key Laboratory of Polymer Materials Engineering (Sichuan University), and the Australian Research Council (ARC) for their continuing support of the project on "Polymer Nanocomposites". Y.W.M. acknowledges the award of an Australian Federation Fellowship by the ARC tenable at the University of Sydney. X.L.X. was also Visiting Professor to the Centre for Advanced Materials Technology (CAMT) at Sydney University supported by the ARC.

**Supporting Information Available:** Experimental details and FTIR, $^1$H NMR, and Raman spectra. This material is available free of charge via the Internet at http://pubs.acs.org.

## References and Notes

(1) (a) Iijima, S. *Nature (London)* **1991**, *354*, 56−58. (b) Ajayan, P. M. *Chem. Rev.* **1999**, *99*, 1787−1790. (c) Baughman, R. H.; Zakhidov, A. A.; de Heer, W. A. *Science* **2002**, *297*, 787−792.

(2) (a) Tasis, D.; Tagmatarchis, N.; Bianco, A.; Prato, M. *Chem. Rev.* **2006**, *106*, 1105−1136. (b) Sun, Y.-P.; Fu, K.; Lin, Y.; Huang, W. *Acc. Chem. Res.* **2002**, *35*, 1096−1104. (c) Balasubramanian, K.; Burghard, M. *Small* **2005**, *1*, 180−192. (d) Banerjee, S.; Hemraj-Benny, T.; Wong, S. S. *Adv. Mater.* **2005**, *17*, 17−29. (e) Hirsch, A. *Angew. Chem., Int. Ed.* **2002**, *41*, 1853−1859.

(3) (a) Xie, X.; Mai, Y.-W.; Zhou, X. *Mater. Sci. Eng. R* **2005**, *49*, 89−112. (b) Qian, D.; Dickey, E. C.; Andrews, R.; Rantell, T. *Appl. Phys. Lett.* **2000**, *76*, 2868−2870. (c) Wei, C.; Srivastava, D.; Cho, K. J. *Nano Lett.* **2002**, *2*, 647−650.

(4) (a) Li, H.; Cheng, F.; Duft, A. M.; Adronov, A. *J. Am. Chem. Soc.* **2005**, *127*, 14518−14524. (b) Hong, C.-Y.; You, Y.-Z.; Pan, C.-Y. *Chem. Mater.* **2005**, *17*, 2247−2254. (c) Buffa, F.; Hu, H.; Resasco, D. E. *Macromolecules* **2005**, *38*, 8258−8263. (d) Hwang, G. L.; Shieh, Y.-T.; Hwang, K. C. *Adv. Funct. Mater.* **2004**, *14*, 487−491.

(5) (a) Baskaran, D.; Mays, J. W.; Bratcher, M. S. *Angew. Chem., Int. Ed.* **2004**, *43*, 2138−2142. (b) Qin, S.; Qin, D.; Ford, W.; Resasco, D. E.; Herrera, J. E. *J. Am. Chem. Soc.* **2004**, *126*, 170−176. (c) Kong, H.; Gao, C.; Yan, D. *J. Am. Chem. Soc.* **2004**, *126*, 412−413. (d) Hong, C.-Y.; You, Y.-Z.; Wu, D.; Liu, Y.; Pan, C.-Y. *Macromolecules* **2005**, *38*, 2606−2611.

(6) (a) Riggs, J. E.; Guo, Z.; Carroll, D. L.; Sun, Y.-P. *J. Am. Chem. Soc.* **2000**, *122*, 5879−5880. (b) Zhao, B.; Hu, H.; Yu, A.; Perea, D.; Haddon, R. C. *J. Am. Chem. Soc.* **2005**, *127*, 8197−8203. (c) Chen, G.-X.; Kim, H.-S.; Park, B. H.; Yoon, J.-S. *J. Phys. Chem. B* **2005**, *109*, 22237−22243.

(7) Liu, Y.; Yao, Z.; Adronov, A. *Macromolecules* **2005**, *38*, 1172−1179.

(8) (a) Zeng, H.; Gao, C.; Yan, D. *Adv. Funct. Mater.* **2006**, *16*, 812−818. (b) Xu, Y.; Gao, C.; Kong, H.; Yan, D.; Jin, Y.; Watts, P. C. P. *Macromolecules* **2004**, *37*, 8846−8853.

(9) (a) Jikei, M.; Kakimoto, M.-A. *Prog. Polym. Sci.* **2001**, *26*, 1233−1285. (b) Gao, C.; Yan, D. *Prog. Polym. Sci.* **2004**, *29*, 183−275. (c) Mori, H.; Müller, A. H. E. *Top. Curr. Chem.* **2003**, *228*, 1−37.

(10) (a) Bergbreiter, D. E.; Tao, G. *J. Polym. Sci., Part A: Polym. Chem.* **2000**, *38*, 3944−3953. (b) Jordan, R.; West, N.; Ulman, A.; Chou, Y.-M.; Nuyken, O. *Macromolecules* **2001**, *34*, 3018−3023.

(11) (a) Bergbreiter, D. E.; Kippenberger, A. M.; Lackowski, W. M. *Macromolecules* **2005**, *38*, 47−52. (b) Muthukrishnan, S.; Erhard, D. P.; Mori, H.; Müller, A. H. E. *Macromolecules* **2006**, *39*, 2743−2750.

(12) Sidorenko, A.; Zhai, X.; Greco, A.; Tsukruk, V. V. *Langmuir* **2002**, *18*, 3408−3412.

(13) Nagale, M.; Kim, B. Y.; Bruening, M. L. *J. Am. Chem. Soc.* **2000**, *122*, 11670−11678.

(14) (a) Bergbreiter, D. E.; Boren, D.; Kippenberger, A. M. *Macromolecules* **2004**, *37*, 8686−8691. (b) Marcos, A. G.; Pusel, T. M.; Thomann, R.; Pakula, T.; Okrasa, L.; Geppert, S.; Gronski, W.; Frey, H. *Macromolecules* **2006**, *39*, 971−977.

(15) (a) Sun, Y.-P.; Huang, W.; Lin, Y.; Fu, K.; Kitaygorodskiy, A.; Riddle, L. A.; Yu, Y. J.; Carroll, L. D. *Chem. Mater.* **2001**, *13*, 2864−2869. (b) Martin, R. B.; Qu, L.; Lin, Y.; Harruff, B. A.; Bunker, C. E.; Gord, J. R.; Allard, L. F.; Sun, Y.-P. *J. Phys. Chem. B* **2004**, *108*, 11447−11453.

(16) Davis, J. J.; Coleman, K. S.; Azamian, B. R.; Bagshaw, C. B.; Green, M. L. H. *Chem.—Eur. J.* **2003**, *9*, 3732−3739.

(17) Sano, M.; Kamino, A.; Shinkai, S. *Angew. Chem., Int. Ed.* **2001**, *40*, 4661−4663.

(18) Campidelli, S.; Sooambar, C.; Diz, E. L.; Ehli, C.; Guldi, D. M.; Prato, M. *J. Am. Chem. Soc.* **2006**, *128*, 12544−12552.

(19) Hwang, S.-H.; Moorefield, C. N.; Wang, P.; Jeong, K.-U.; Cheng, S. Z. D.; Kotta, K. K.; Newkome, G. R. *J. Am. Chem. Soc.* **2006**, *128*, 7505−7509.

(20) Wang, X.; Liu, H.; Jin, Y.; Chen, C. *J. Phys. Chem. B* **2006**, *110*, 10236−10240.

(21) (a) Holzinger, M.; Abraham, J.; Whelan, P.; Graupner, R.; Ley, L.; Hennrich, F.; Kappes, M.; Hirsch, A. *J. Am. Chem. Soc.* **2003**, *125*, 8566−8580. (b) Star, A.; Stoddart, J. F. *Macromolecules* **2002**, *35*, 7516−7520.

(22) Schlüter, A. D.; Rabe, J. P. *Angew. Chem., Int. Ed.* **2000**, *39*, 864−883.

(23) (a) Hilliou, L.; Vlassopoulos, D.; Rehahn, M. *Macromolecules* **1998**, *31*, 1406−1417. (b) Wegner, G. *Macromol. Chem. Phys.* **2003**, *204*, 347−357. (c) Zhang, L.; Eisenberg, A. *J. Am. Chem. Soc.* **1996**, *118*, 3168−3181.

(24) Sano, M.; Kamino, A.; Okamura, J.; Shinkai, S. *Langmuir* **2001**, *17*, 5125−5128.

(25) Lu, Y.; Yang, X.; Ma, Y.; Du, F.; Liu, Z.; Chen, Y. *Chem. Phys. Lett.* **2006**, *419*, 390−393.

(26) Yang, Y.; Xie, X.; Wu, J.; Mai, Y.-W. *J. Polym. Sci., Part A: Polym. Chem.* **2006**, *44*, 3869−3881.

(27) Gao, C. *Macromol. Rapid Commun.* **2006**, *27*, 841−847.

(28) (a) Mitchell, C. A.; Bahr, J. L.; Arepalli, S.; Tour, J. M.; Krishnamoorti, R. *Macromolecules* **2002**, *35*, 8825−8830. (b) Pötschke, P.; Fornes, T. D.; Paul, D. R. *Polymer* **2002**, *43*, 3247−3255.

(29) (a) Kim, B.; Park, H.; Sigmund, W. M. *Colloids Surf., A* **2005**, *256*, 123−127. (b) Grunlan, J. C.; Liu, L.; Kim, Y. S. *Nano Lett.* **2006**, *6*, 911−915.

(30) Yang, Y.; Xie, X.; Wu, J.; Yang, Z.; Wang, X.; Mai, Y.-W. *Macromol. Rapid Commun.* **2006**, *27*, 1695−1701.

(31) Bartelink, C. F.; De Pooter, M.; Grünbauer, H. J. M.; Beginn, U.; Möller, M. *J. Polym. Sci., Part A: Polym. Chem.* **2000**, *38*, 2555−2565.

(32) Chen, J.; Hamon, M. A.; Hu, H.; Chen, Y.; Rao, A. M.; Eklund, P. C.; Haddon, R. C. *Science* **1998**, *282*, 95−98.

(33) Chen, R. J.; Zhang, Y.; Wang, D.; Dai, H. *J. Am. Chem. Soc.* **2001**, *123*, 3838−3839.
(34) Baskaran, D.; Mays, J. W.; Zhang, X.; Bratcher, M. S. *J. Am. Chem. Soc.* **2005**, *127*, 6916−6917.
(35) Tang, B.; Xu, H. *Macromolecules* **1999**, *32*, 2569−2576.
(36) Hawker, C. J.; Lee, R.; Fréchet, J. M. J. *J. Am. Chem. Soc.* **1991**, *113*, 4583−4588.
(37) Flory, P. J. *J. Am. Chem. Soc.* **1952**, *74*, 2718−2723.
(38) Hanselmann, R.; Hölter, D.; Frey, H. *Macromolecules* **1998**, *31*, 3790−3901.
(39) Hölter, D.; Frey, H. *Acta Polym.* **1997**, *48*, 298−309.
(40) Radke, W.; Litvinenko, G.; Müller, A. H. E. *Macromolecules* **1998**, *31*, 239−248.
(41) Yan, D.; Müller, A. H. E.; Matyjaszewski, K. *Macromolecules* **1997**, *30*, 7024−7033.
(42) Yamakawa, Y.; Ueda, M.; Takeuchi, K.; Asai, M. *Macromolecules* **1999**, *32*, 8363−8369.
(43) Wang, C.-F.; Su, Y.-C.; Kuo, S.-W.; Huang, C.-F.; Sheen, Y.-C.; Chang, F.-C. *Angew. Chem., Int. Ed.* **2006**, *45*, 2248−2251.
(44) Hirashima, Y.; Sato, H.; Suzuki, A. *Macromolecules* **2005**, *38*, 9280−9286.
(45) Uppuluri, S.; Keinath, S. E.; Tomalia, D. A.; Dvornic, P. R. *Macromolecules* **1998**, *31*, 4498−4510.
(46) Farrington, P. J.; Hawker, C. J.; Fréchet, J. M. J.; Mackay, M. E. *Macromolecules* **1998**, *31*, 5043−5050.
(47) Nunez, C. M.; Chiou, B.-S.; Andrady, A. L.; Khan, S. A. *Macromolecules* **2000**, *33*, 1720−1726.
(48) (a) Naylor, A. M.; Goddard, W. A.; Kiefer, G. E., III; Tomalia, D. A. *J. Am. Chem. Soc.* **1989**, *111*, 2339−2341. (b) Murat, M.; Grest, G. S. *Macromolecules* **1996**, *29*, 1278−1285.
(49) (a) Fréchet, J. M. J. *Science* **1994**, *263*, 1710−1715. (b) Hawker, C. J.; Farrington, P. J.; Mackay, M. E.; Wooley, K. L.; Fréchet, J. M. J. *J. Am. Chem. Soc.* **1995**, *117*, 4409−4410.
(50) Sendijarevic, I.; McHugh, A. J. *Macromolecules* **2000**, *33*, 590−596.
(51) Otsubo, Y. *Langmuir* **1999**, *15*, 1960−1965.
(52) (a) Tam, K. C.; Jenkins, R. D.; Winnik, M. A.; Bassett, D. R. *Macromolecules* **1998**, *31*, 4149−4159. (b) Vittadello, S. T.; Biggs, S. *Macromolecules* **1998**, *31*, 7691−7697. (c) Smith, G. L.; McCormick, C. L. *Macromolecules* **2001**, *34*, 5579−5586.
(53) Witten, T. A.; Cohen, M. H., Jr. *Macromolecules* **1985**, *18*, 1915−1918.
(54) (a) Marrucci, G.; Bhargava, S.; Cooper, S. L. *Macromolecules* **1993**, *26*, 6483−6488. (b) Ma, S. X.; Cooper, S. L. *Macromolecules* **2001**, *34*, 3294−3301.
(55) Noda, T.; Hashidzume, A.; Morishima, Y. *Langmuir* **2000**, *16*, 5324−5332.
(56) (a) Eliassaf, J.; Silberberg, A.; Katchalsky, A. *Nature (London)* **1955**, *4493*, 1119−1203. (b) Hu, Y.; Wang, S. Q.; Jamieson, A. M. *Macromolecules* **1995**, *28*, 1847−1853.
(57) Ait-Kadi, A.; Carreau, P. J.; Chauveteau, G. *J. Rheol.* **1987**, *31*, 537−561.
(58) Hansson, P.; Lindman, B. *Curr. Opin. Colloid Interface Sci.* **1996**, *1*, 604−610.
(59) Liu, R. C. W.; Morishima, Y.; Winnik, F. M. *Macromolecules* **2001**, *34*, 9117−9124.
(60) Hirashima, Y.; Sato, H.; Suzuki, A. *Macromolecules* **2005**, *38*, 9280−9286.
(61) (a) Lyulin, A. V.; Adolf, D. B.; Davies, G. R. *Macromolecules* **2001**, *34*, 3783−3789. (b) Thompson, D. S.; Markoski, L. J.; Moore, J. S.; Sendijarevic, I.; Lee, A.; McHugh, A. J. *Macromolecules* **2000**, *33*, 6412−6415. (c) Magnusson, H.; Malmstrom, E.; Hult, A.; Johansson, M. *Polymer* **2002**, *43*, 301−306.
(62) Hawker, C. J.; Chu, F. *Macromolecules* **1996**, *29*, 4370−4380.
(63) (a) McCormick, C. L.; Middleton, J. C.; Cummins, D. F. *Macromolecules* **1992**, *25*, 1201−1206. (b) Volpert, E.; Selb, J.; Candau, F. *Macromolecules* **1996**, *29*, 1452−1463.
(64) Badiger, M. V.; Rajamohanan, P. R.; Suryavanshi, P. M.; Ganapathy, S.; Mashelkar, R. A. *Macromolecules* **2002**, *35*, 126−134.

MA0707077